Journal of Statistical Physics, Vol. 21, No. 4, 1979

On the Hénon–Pomeau Attractor

Carles Simó[1]

Received January 24, 1979

The behavior of the iterates of the map $T(x, y) = (1 + y - ax^2, bx)$ can be useful for the understanding of turbulence. In this study we fix the value of b at 0.3 and allow a to take values in a certain range. We begin with the study of the case $a = 1.4$, for which we determine the existence of a strange attractor, whose region of attraction and Hausdorff dimension are obtained. As we change a, we study numerically the existence of periodic orbits (POs) and strange attractors (SAs), and the way in which they evolve and bifurcate, including the computation of the associated Lyapunov numbers. Several mechanisms are proposed to explain the creation and disappearance of SAs, the basin of attraction of POs, and the cascades of bifurcations of POs and of SAs for increasing and decreasing values of a. The role of homoclinic and heteroclinic points is stressed.

KEY WORDS: Hénon–Pomeau attractor; evolution of strange attractors; Hausdorff dimension; Lyapunov numbers; numerical experiments; homoclinic and heteroclinic points.

1. INTRODUCTION

The attempt to understand the nature of turbulence has led to the introduction of simplified problems exhibiting a behavior similar to that of the actual case —for example, use of the Lorenz equations[11] as a model of the Bénard problem. The Poincaré map associated with the Lorenz equations led Hénon and Pomeau[7] to introduce the "easiest" nontrivial map from R^2 into itself. It is easy in the sense that the equations are quadratic and the Jacobian is constant (a Cremona map). Furthermore, all the Cremona quadratic maps can be put into the form used by Hénon and Pomeau. This map is a model of the Poincaré map associated with the Lorenz equations with some magnification of the Jacobian in order to see the structure.

[1] Facultat de Matemàtiques, Universitat de Barcelona, Spain.

0022-4715/79/1000-0465$03.00/0

1.1. The Equations and Fixed Points

The map introduced by Hénon and Pomeau is given through the equation $T(x, y) = (1 + y - ax^2, bx)$. We have $|DT| = -b$, and we fix from now on the value $b = 0.3$.[5,7] We note that T is orientation-reversing. In some cases the use of T^2 instead of T is more convenient.

The fixed points of T are $H_\pm$ with coordinates $x_\pm = \{-(1-b) \pm [(1-b)^2 + 4a]^{1/2}\}/2a$, $y_\pm = bx_\pm$. We shall call the set of points for which $|x| < (1-b)/2a$ the contractive zone. As $DT = \begin{pmatrix} -2ax & 1 \\ b & 0 \end{pmatrix}$, the eigenvalues at $H_\pm$ are $\lambda = -ax \pm (a^2x^2 + b)^{1/2}$. We see that H_- will be a saddle point for all values of a. The point H_+ will be in the contractive zone and hence asymptotically stable for small values of $a > 0$. For $a = 3(1-b)^2/4$, H_+ is in the boundary of the contractive zone and we have $\lambda = -1$. [At this point a bifurcation to two 2-periodic points appears, which are stable up to $a = (1-b)^2 + (1+b)^2/4$, when a 4-periodic orbit bifurcates.] For larger values of a, H_+ leaves the contractive zone and is a saddle point. Notice that if $a > (3 - 2b - b^2)/4$ no more than two successive points lie in the contractive zone.

1.2. Invariant Manifolds

The invariant manifolds of the hyperbolic points are obtained in an elementary way. Let $y = \phi(x)$ be their equation near the fixed point and (f, g) the components of T. We impose $g(x, \phi(x)) = \phi(f(x, \phi(x)))$. Let β_1 be the linear part of ϕ, given by the eigenvalues of DT at the fixed points. Consider the sequence $\{\beta_n\}$ defined recursively by

$$\beta_1 = ax_0 \pm (a^2x_0^2 + b)^{1/2}; \qquad \beta_2 = a\beta_1/(\beta_1 + \gamma_1^2)$$

$$\beta_3 = -2\beta_2\gamma_1\gamma_2/(\beta_1 + \gamma_1^3)$$

$$\beta_4 = -[\beta_2(\gamma_2^2 + 2\gamma_1\beta_3) + 3\beta_3\gamma_1^2\gamma_2]/(\beta_1 + \gamma_1^4)$$

$$\beta_5 = -[\beta_2(2\gamma_1\beta_4 + 2\gamma_2\beta_3) + \beta_3(3\gamma_1\gamma_2^2 + 3\gamma_1^2\beta_3) + 4\beta_4\gamma_1^3\gamma_2]/(\beta_1 + \gamma_1^5)$$

$$\beta_6 = -[\beta_2(2\gamma_1\beta_5 + 2\gamma_2\beta_4 + \beta_3^2) + \beta_3(3\gamma_1^2\beta_4 + 6\gamma_1\gamma_2\beta_3 + \gamma_2^3) + \beta_4(4\gamma_1^3\beta_3 + 6\gamma_1^2\gamma_2^2) + 5\beta_5\gamma_1^4\gamma_2]/(\beta_1 + \gamma_1^6)$$

$$\vdots$$

where we have introduced $\gamma_1 = \beta_1 - 2ax_0 = b/\beta_1$, $\gamma_2 = \beta_2 - a = -a\beta_1^5/[b^2(\beta_1^3 + b^2)]$; (x_0, y_0) is one of the fixed points.

The stable and unstable invariant manifolds W_+^s, W_+^u (resp. W_-^s, W_-^u) of H_+ (resp. H_-) have the common expression $\eta = \phi(\xi) = \sum_{i \geq 1} \beta_i \xi^i$, where $\xi = x - x_0$ and $\eta = y - y_0$. Due to the hyperbolicity of $H_\pm$ the radius of convergence of ϕ is positive.

Given a segment of an unstable invariant manifold we globalize by iteration[16]: Select a value ξ_1 such that $\xi_2 = \beta_1{}^2\xi_1$ is in the region of convergence and some spacing $h = (\xi_2 - \xi_1)/n$ (n is not necessarily an integer). First we obtain the images of $\xi = \xi_1 + kh$, $k = 0$ to $n - 1$ under T^s, $s = 2$. When ξ reaches ξ_2, both ξ and h are divided by $\beta_1{}^2$ and s is increased by 2. This procedure is iterated as necessary. Use T^{-1} for the stable manifolds.

The same method can be applied in order to find the invariant manifolds $W^{s,u}_{n\text{-PO}}$ of a point in an n-periodic orbit (n-PO) which is hyperbolic under T^n. However, the expression for T^n is rather cumbersome: polynomials of degree 2^n. We remind the reader that following Poincaré the points in $W^s_{n\text{-PO}} \cap W^u_{m\text{-PO}}$ are called homoclinic if the POs are the same and heteroclinic if they are different.

In a similar way we can find the asymptotic expansion of the unbounded branches of $W_+{}^s$ and $W_-{}^u$ when x tends toward $+\infty$ and $-\infty$, respectively. They are

$$y = ax^2 + \left(\frac{b}{a}\right)^{1/2} x^{1/2} - 1 - \frac{(b/a)^{1/4}/(2a)}{(b/16a^5)^{1/4}}\, x^{-1/4} + o(x^{-1/4})$$

and

$$y = -(b/a)^{1/2}(-x)^{1/2} + \left(\frac{b^8}{16a^5}\right)^{1/4}(-x)^{-1/4} + o(x^{-1/4})$$

Parts of this work, in particular Section 2, were presented previously.[15] Some comments of Dr. Hénon have stimulated the search for a more complete description of the family of diffeomorphisms.

2. THE FIRST EXAMPLE

The case $a = 1.4$ has the historical importance of being the first analyzed by Hénon and Pomeau. They discovered the existence of a strange attractor, i.e., an attractor that is neither a fixed point nor an attracting PO. It is instructive to study this case first.

2.1. Stable and Unstable Regions

Figure 1 shows qualitatively the invariant manifolds of H_+ and H_-. For a more quantitative point of view of the strange attractor we refer to Refs. 5 and 7, but the smallness of some details does not allow us to see the structure.

The two branches of W^s_- are the boundary of a region R which contains H_+ (and, of course, one of the branches of W^u_-). Both branches tend toward W^s_+ by iteration of T^{-1}. The measure of R is unbounded and the tongues

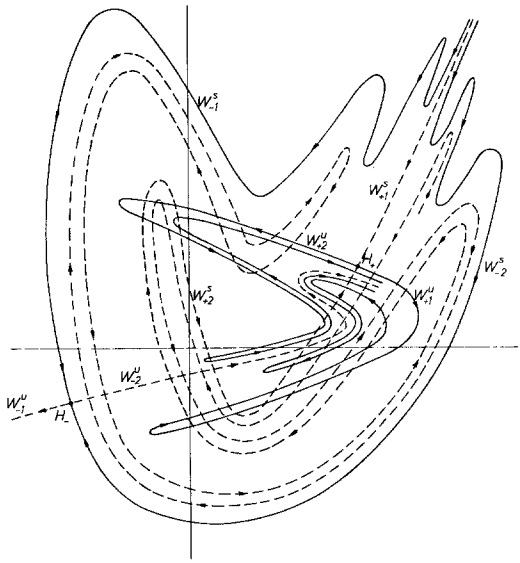

Fig. 1. $a = 1.4$: Qualitative picture of the invariant manifolds of the fixed points.

formed by W^s_- become finer when $x \to +\infty$.[5] (For an area-preserving diffeomorphism this will be equivalent to the existence of a nonisolating integral.)

The behavior of the two branches of W^s_+ is quite different. One of them, W^s_{+1}, has no turning points and has the asymptotic expansion given in Section 1.2. The other one oscillates around both sides of W^s_{+1}, approaching W^s_-, and reproduces the structure of the fine tongues.

With respect to unstable manifolds, one of the branches, W^u_{-1}, of W^u_- has no turning points and approaches $-\infty$ asymptotically, as has been described in Section 1. Through iterates T^k the points outside R pass from the vicinity of W^s_{+1} for $k \to -\infty$ to that of W^u_{-1} for $k \to +\infty$.

The two branches of W^u_+ are inclosed in R and, in fact, if we cut by a convenient disk centered at the origin (of radius 100, say), in an invariant bounded set. Other invariant bounded sets are given in Refs. 5 and 7. Both branches are interlaced and between them we find the unstable bounded branch W^u_{-2} of W^u_-.

2.2. Homoclinic and Heteroclinic Points

Figure 2 shows, again qualitatively, some of the first tongues of W^u_{+1}, including homoclinic points belonging to $W^u_{+1} \cap W^s_{+2}$. As noted in Ref. 3, the computation of iterates is severely beset by errors (exponentially growing), but we can have confidence in the "first" homoclinic point. Actually the exponential growth is produced along W^u and not across the manifold (see

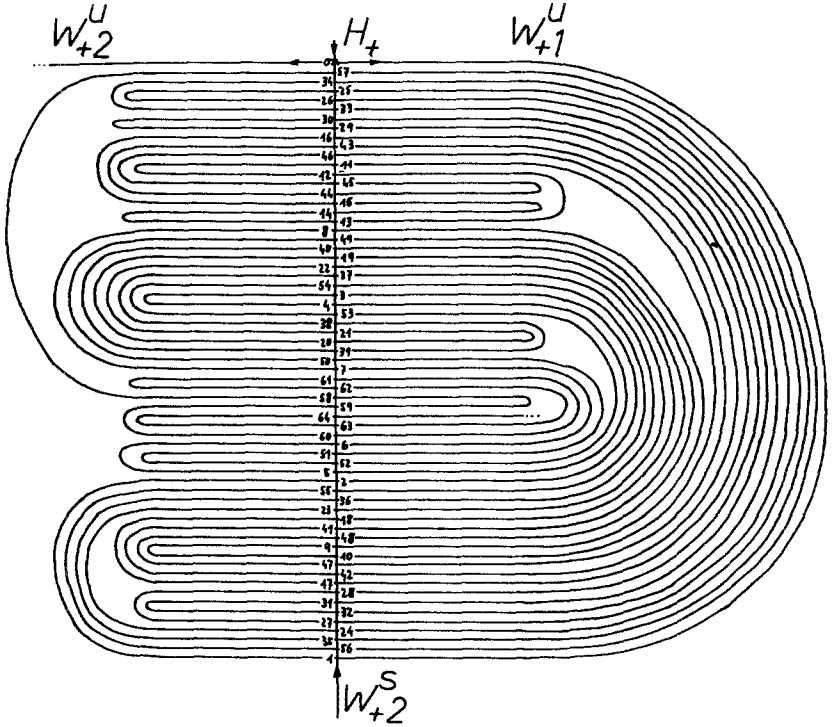

Fig. 2. $a = 1.4$: Qualitative behavior of W^u_{+1}, showing some of the homoclinic points (64) and their order on W^s_{+2}.

below for the discussion of Lyapunov numbers). We can say that the W^u produced is correct but the parametrization is not.

The information given in Fig. 2 is part of a computation of homoclinic points reduced to the segment of W^s_{+2} between H_+ and the Y axis. Using the method described in Section 1.2, we obtain the first 500 homoclinic points starting with $\xi_1 = 0.001$ and $n \simeq 37$. At most 24 iterations of T are needed. Then we order the homoclinic points along W^s_{+2} by increasing ordinate. The impossibility of seeing the fine structure in a plot is illustrated by the fact that the distance between the homoclinic points numbers 500 and 473 (consecutive in W^s_{+2}) is 2.9×10^{-14}. Table I gives the 25 first homoclinic points. Such points and many others will be used in Section 2.5.

The images under T (note that T preserves orientation along W^s_{+2}) of the computed homoclinic points belong to $W^u_{+2} \cap W^s_{+2}$. Between two families we have heteroclinic points belonging to $W^u_{-2} \cap W^s_{+2}$. We call such points inner heteroclinic. Another kind, which we shall call outer heteroclinic points, plays a very important role, which will be studied in Section 4.1.

Table I. First Homoclinic Points in $W^s_{+2} \cap W^u_{+1}$ for $a = 1.4$

x	y
0.338644551953	−0.255139766232
0.340827035075	−0.252591279980
0.623951842734	0.175241370201
0.602042198865	0.134205149735
0.431432347190	−0.139902534849
0.431437264629	−0.139895795582
0.602009451523	0.134144808379
0.624011863858	0.175355611563
0.340778644025	−0.252757403588
0.338890064418	−0.254866334584
0.631174277631	0.189059731319
0.630638901288	0.188030470072
0.626361920241	0.179836428241
0.626362046392	0.179836669182
0.630638098792	0.188028927867
0.631175740094	0.189062543991
0.338886968299	−0.254869783827
0.340782406880	−0.252753191830
0.624007963876	0.175348188219
0.602018383611	0.134161266651
0.602030951824	0.134184425224
0.623958299271	0.175253658789
0.340919750369	−0.252599436624
0.338652367403	−0.255131064599
0.631350094671	0.189397912524

2.3. Attracting Character

As $|DT^2| = b^2 = 0.09$ and $\lambda^2 \simeq 3.7$ along W^u_{+1}, the initial errors in points used to generate W^u_{+1} are quickly reduced. Locally (near H_+) W^u_+ is an attracting manifold. (However, at some points, especially near the end of the fine tongues of W^u_+, it is possible to find that DT^2 is contracting along the manifold and expanding in directions transverse to it. That this is not the average case is discussed in Section 5.1.) The fact that W^u_+ cuts the contracting zone $|x| < 0.25$ may play a role in the attracting character of W^u_+.

The most important feature in order that W^u_+ be an attractor is the existence of homoclinic points. When a point near H_+ is attracted by W^u_+ their images are near W^u_+ and the average distance to W^u_+ is reduced by a factor of ~ 0.2 at every iteration under T. The presence of homoclinic points

Table II. Some Periodic Points for $a = 1.4$

n	x	y
2	−0.47580004	0.29274002
4	0.21776177	0.19145820
6	0.24331390	0.24084051
	0.31145232	0.17386310
7	0.12844340	0.25534765
	0.21789019	0.24541056
	0.36788265	0.20824060
	0.37068442	0.19237492
8	0.10042074	0.25936957
	0.23400077	0.24377027
	0.27904750	0.18033354
	0.36859296	0.22487145
	0.40329615	0.21137377
	0.40447097	0.17838995
	0.43962159	0.17060379
9	0.11635251	0.25773957
	0.40320219	0.22102278
10	0.17985526	0.19826568
	0.20759334	0.19388329
	0.23059169	0.24423380
	0.28974097	0.17821733
	0.32749477	0.23023617
	0.43732151	0.21626365
	0.46710699	0.21213436
11	0.32655413	0.23190253
12	0.07528779	0.26074152
	0.02154057	0.26678955
13	0.11206125	0.24040817
	0.44024457	0.21723486
14	0.14584542	0.25330918
	0.20381413	0.21857411
15	0.07932553	0.21593891
	0.25918394	0.18361096
17	0.30688114	0.22294060
18	0.31439051	0.22119578
19	0.16520045	0.25029259
	0.44276055	0.21551536
20	0.02198433	0.26842848
	0.19104625	0.24897300
21	0.02825633	0.26736014
	0.07927680	0.26176091
23	0.30521445	0.20929979
24	0.18111044	0.24994053

produces a feedback and (perhaps after a great number of iterations) the point returns to the neighborhood of H_+. For points attracted initially by W^u_{-1} the role of the homoclinic points is played by the inner heteroclinic ones. After some iterations they come near W^u_+.

From the numerical experiments done with the $a = 1.4$ value it seems that almost every point in R is attracted by W^u_+, which then becomes (part of) a strange attractor. The exceptions are the periodic points. So far none of the computed POs is attracting. The importance of attracting POs is discussed in Section 4.3. Table II gives some of the periodic points for $a = 1.4$. It seems that the only periods not present are 3 and 5. We study both cases in Section 3.2.

2.4. Periodic Points

The equation for an n-periodic point is $T^n(x_0, y_0) = (x_0, y_0)$, or, equivalently, in R^n, $x_{k+1} - bx_{k-1} - ax_k^2 = 0$, $k = 1$ to n, with $x_i = x_j$ if $i \equiv j \pmod n$. Every one of the n equations represents a hypercylinder with $(n-2)$-dimensional generatrix and has as orthogonal cross section a parabola in a plane generated by vectors of the form $(1, 0, \ldots, 0)^T$ and $(0, 1, 0, \ldots, -b)^T$ (for the remaining equations apply circular permutation). All the parabolas are equal.

Let $F(x) = 0$ be the set of n equations defining the n-periodic points. According to Bézout's theorem the number of solutions (in $\mathbb{C}^n$) is 2^n if all the components of $F(x) = 0$ are zero-dimensional. Let us suppose that a one-dimensional component V exists and that $x, y \in V$ with $\|x - y\|$ small enough. Then

$$0 = F(y) = F(x) + DF(x)(y - x) + 0.5D^2F(x)(x - y)^2$$

$DF(x)(y - x)$ can be zero if x is a double point, but if I_n is the identity matrix in R^n, then D^2F is aI_n, a scalar matrix, which leads to an absurdity if $x \neq y$. So, we have at most 2^n real n-periodic points. For Sections 3 and 4 it is interesting to analyze double points (i.e., bifurcation points).

The $n + 1$ equations giving a bifurcation are $F(x, a) = 0$, $|D_xF(x, a)| = 0$ (where we make it explicit that a is a parameter). The last equation can also be written $0 = |DT^n - I| = (-b)^n - \mathrm{Tr}(DT^n) + 1$. If we expand we get

$$0 = (2a)^n \sum_n + (2a)^{n-2}b \sum_{n,1} + (2a)^{n-4}b^2 \sum_{n,2} + \cdots$$

$$+ (2a)^{n-2[n/2]}b^{[n/2]} \sum_{n,[n/2]} - (-b)^n - 1$$

where $\sum_n = \sum_{i=1}^n x_i$ and $\sum_{n,k}$ is the sum of all the products of $n - 2k$ factors obtained by taking off from $x_1,\ldots, x_n$, considered circularly, k couples of consecutive elements. For instance,

$$\sum_{6,2} = x_1x_2 + x_2x_3 + x_3x_4 + x_4x_5 + x_5x_6 + x_6x_1 + x_1x_4 + x_2x_5 + x_3x_6$$

It is curious to note that the number of elements in $\sum_{n,k}$ is

$$V_k(n) = \frac{n}{n-k}\binom{n-k}{k}$$

a number closely related to the classical "problème des ménages" in combinatorial analysis!

The unstable POs have invariant manifolds $W^s_{n\text{-PO}}$ and $W^u_{n\text{-PO}}$. Roughly speaking, the unstable manifolds $W^u_{n\text{-PO}}$ are "parallel" to W^u_+ and the $W^s_{n\text{-PO}}$ are transverse to it. There are heteroclinic points, which implies that $W^u_{n\text{-PO}} \subset \overline{W^u_+}$. Then the strange attractor is really the closure of W^u_+. We shall call such an attractor the Hénon–Pomeau attractor.

2.5. Cantorian Character and Hausdorff Dimension

It is well known that the introduction of the "horseshoe diffeomorphism"[16] has been very fruitful in the study of the vicinity of the homoclinic (or heteroclinic) points through symbolic dynamics.

In our case we shall use similar techniques in order to study the Cantorian character, and at the same time we shall compute the Hausdorff dimension of W^u_{+1}. The Hausdorff dimension[8] is a convenient tool for the description of sets "intermediate" between a point and a segment, such as the ternary set of Cantor.

We consider W^u_{+1} and its intersection by W^s_{+2}. Because of the stable character of the latter, every point tends to H_+ under T^k, $k \to \infty$. We consider the points B, C,..., I, J (see Fig. 3). All of them are mapped in $\overline{AH}_+$ by T^4. Moreover, through the components of W^u_{+1} that intersect W^s_{+2} between A and H_+, a feedback is produced. We shall say that $\overline{AH}_+$ is mapped in $\overline{BC}$, $\overline{DE}$, $\overline{FG}$, $\overline{IJ}$. This allows us to idealize and to propose the following model.

Model I. $\overline{AH}_+$ is mapped in $\overline{BC}$, $\overline{DE}$, $\overline{FG}$, $\overline{IJ}$, which in turn are mapped by T^4 in $\overline{B'C'}$,..., $\overline{I'J'}$, $B' \equiv A$, all of which are in $\overline{AH}_+$. We assume that the four images $\overline{B'C'}$, etc. are obtained linearly from $\overline{AH}_+$ by mappings ϕ_i, $i = 1$–4, and that in $\overline{AH}_+$ the mapping T^2 is linear. Then $W^u_{+1} \cap \overline{AH}_+$ is a Cantor set and its Hausdorff dimension is the value of α that satisfies

$$\lambda^\alpha + \sum_{i=1}^{4} l_i^\alpha = 1 \quad \text{with} \quad \lambda = d(T^2X, H_+)/d(X, H_+)$$

where X is any point of $\overline{AH}_+$ and $l_1 = d(B', C')/d(A, H_+)$, $l_2 = d(D', E')/d(A, H_+)$, etc.

It is sufficient to study the intervals that will be eliminated from $\overline{AH}_+$ by the successive feedbacks and applications of T^2.

First we suppress $\overline{C'D'}$, $\overline{E'F'}$, $\overline{G'I'}$, $\overline{J'T^2B'}$ and their images under T^{2j}, $j > 0$ (an infinite set of intervals, which makes a difference with respect to the ternary Cantor set).

Second, we supress in $\overline{B'C'}$, $\overline{D'E'}$, $\overline{F'G'}$, $\overline{I'J'}$ the images ξ under ϕ_i, $i = 1$–4, of the intervals eliminated by the first operation and the images under T^{2j}, $j > 0$, of the components of ξ, etc. It is clear because of the linearity of T^2 and of ϕ_i that one obtains a Cantor set.

With respect to the Hausdorff measure, using the Besicovitch–Taylor relation[8] (which gives the dimension for Cantor sets if we take $\inf \alpha$), it is sufficient to determine $\inf \alpha$ for the α such that the sum of the powers α for the suppressed intervals is finite. But this sum is a geometrical progression of ratio $\sum_{i=1}^4 l_i^\alpha \sum_{j \geqslant 0} \lambda^{j\alpha}$. We must have $\sum_{i=1}^4 l_i^\alpha/(1 - \lambda^\alpha) < 1$ and in going to inf we obtain the desired relation.

Application. We have already obtained the first 500 intersections of W^u_{+1} with the part $\overline{BH}_+$ of W^s_{+2} (Fig. 3). This gives in particular the points $A', \ldots, J'$ and one obtains the numerical values $\lambda^{-1} = 41.11968$; $l_i^{-1} = 1145.6$, 1896, 58670, 9230, respectively. Therefore $\alpha \simeq 0.2303$.

However, model I does not agree completely with reality, as has been noted. A first modification consists in not considering the applications ϕ_i as linear. The length of the intervals suppressed at each feedback depends on the nonlinearity. If ϕ_i is (r_i, R_i)-Lipschitz (i.e., $r_i|a - b| \leqslant |f(a) - f(b)| \leqslant R_i|a - b|$), we can prove immediately that $\alpha \in [\alpha_1, \alpha_2]$ with

$$\sum (r_i l_i)^{\alpha_1} + \lambda^{\alpha_1} = 1 = \sum (R_i l_i)^{\alpha_2} + \lambda^{\alpha_2}$$

In our case the limitations $0.5 < r_i < R_i < 2$ imply $\alpha \in [0.2167, 0.2461]$ and $0.1 < r_i < R_i < 10$ imply $\alpha \in [0.1915, 0.2959]$.

In reality things are more complex. Figure 3 shows qualitatively the type of thing that happens. The different loops of W^u_{+1} can intersect W^s_{+2} between A and H_+, say in points M and N, and, for instance, not intersect W^s_{+2} between D and E. This implies for the corresponding ϕ (in this case ϕ_2) that points far apart such as M^*, N^* of $\overline{AH}_+$ are mapped in much closer points on $\overline{DE}$ (the value of r_i should be taken as 0). As a result, the Cantor set increases (because of the absence of feedback from the suppressed intervals).

Model II. The applications ϕ_i of model I are not defined in some subintervals of $\overline{AH}_+$ (see Fig. 3). However, it is possible to come back to model I by considering not the direct feedback on $\overline{BC}$, $\overline{DE}$, etc., but the feedback after a number of foldings of W^u_{+1}.

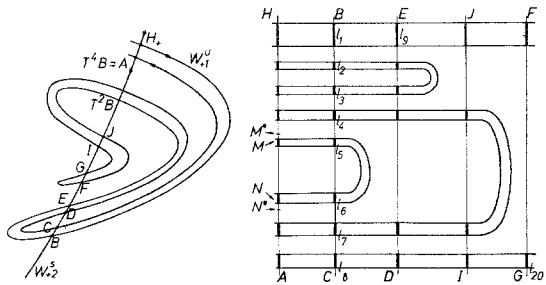

Fig. 3. $a = 1.4$: The feedback effect, models I and II, for the Cantorian character of the SA and for the evaluation of the Hausdorff dimension.

Application. As indicated in Fig. 3, one obtains now 20 different images for the ϕ_i. We assume again linearity (which is accurate enough). We obtain the values of l_i^{-1}: $1.338E6$, $3.15E8$, $1.39E9$, $4.176E6$, $5.777E6$, $1.083E7$, $2.101E6$, $1.152E6$, $1.289E6$, $2.77E8$, $0.825E9$, $3.809E6$, $2.342E6$, $1.195E6$, $0.996E6$, $1.111E6$, $1.057E6$, $1.047E6$, $4.855E5$, $4.916E5$, considering the images under T^4 in $\overline{AH}_+$. Therefore $\alpha \simeq 0.2365$, and we see that our initial estimate was not too erroneous.

Of course, considering the feedback in successive steps, one can build models which approach the reality more and more closely.

With respect to W^u_{+2}, since it is TW^u_{+1} and T is linear on W^s_{+2} in the vicinity of H_+ (approximately), the Hausdorff dimension of $W^u_{+2} \cap W^s_{+2}$ will be the same as that of $W^u_{+1} \cap W^s_{+2}$. Finally, W^u_{-2} is inserted between the two branches of W^u_+, and, in the absence of a more detailed study, does not seem to bring any essential modification to the above description. Therefore the Hausdorff dimension of the attractor will be the value obtained for W^u_{+1}.

We have seen that in the computation of the Hausdorff dimension there are two facts to take into account: the eigenvalue at H_+ along W^s_+ and the feedback effect of the unstable manifold.

The inclusion of $W^u_{n\text{-PO}}$ is not necessary in the computation of the Hausdorff dimension. If it is true that for $a = 1.4$ all the POs are unstable, then the corresponding λ along $W^s_{n\text{-PO}}$ are less than 0.3^n. The Hausdorff dimension of $W^u_{n\text{-PO}}$ (provided that there are homoclinic points) decreases when n increases. As the Hausdorff dimension of a union is the greatest dimension of the components, the only dimension to take into account is that of W^u_+.

3. NUMERICAL EXPERIMENTS

Following the study of the case $a = 1.4$ we undertake the cases $a > 1$. As noted by Feit,[5] for values of a greater than 1.4269... it is difficult to see

any attractor, with some minor exceptions. First we compute attractors for $a = 1(0.01)1.42$.

3.1. Some Attractors

The method followed to detect attractors for every value of a consists in taking as initial points $x = 0(0.1)1$, $y = -0.3(0.1)0.3$, computing the first 4000 iterates of every point, and plotting the following 1000 iterates. We list the results with comments:

$a = 1.00$–1.02: 4-periodic attractor. The four points are roughly on a parabola like the part of W^u_+ in Section 2 between the first fine tongues.

1.03–1.05: 8-periodic attractor. There are four groups of two points. The distance between couples increases when a does.

1.06: Eight pieces of strange attractor (SA). Each piece is roughly centered in an 8-periodic unstable point.

1.07: Four pieces of SA and a 6-periodic attractor. Each one of the pieces seems to be the fusion of two pieces of the preceding case. Centered in 4-periodic unstable points.

1.08: Four pieces of SA on one side and six pieces of SA on the other. The six pieces substitute the 6-periodic attracting orbit.

1.09–1.15: Two pieces of SA. Each one is obtained by the fusion of two pieces of the preceding case. When a increases, each piece suffers folding and increases in amplitude.

1.16–1.22: One SA obtained by fusion of the two preceding pieces. Folding increases if a does.

1.23–1.25: 7-periodic attractor. The seven points are disposed on a curve which reminds one of the preceding SA.

1.26: 14-periodic attractor. There are seven pairs of points. Each pair replaces one of the seven points.

1.27: Seven pieces of SA, each one centered in a 7-periodic unstable point.

1.28–1.29: One SA. With some more folding we find again the attractor obtained for $a = 1.16$–1.22.

1.30: 7-periodic attractor. The same comment as for $a = 1.23$–1.25.

1.31–1.42: One SA. Some comment as for $a = 1.28$–1.29.

Many questions can be formulated: Some bifurcations of POs are clear, but the appearance of SAs, their fusion, their disappearance, the coexistence

of different attractors, and why an attracting PO sometimes destroys a SA and sometimes does not, are a challenge. In Section 4 we attempt to give mechanisms for explaining such phenomena and the ones to be encountered in the following numerical experiments.

3.2. Periodic Orbits: Evolution and Bifurcations

The computation of POs for a given value of a is a hard task. Except for small values of the period, it is cumbersome to write the adequate polynomial. We have used minimization and quasi-Newton methods in order to get some periodic points. After a PO is obtained we obtain its evolution by the continuation or Davidenko method.

Let $G(x, y, a) = T_a^n(x, y) - (x, y)$. We must have $G(x, y, a) = 0$. Introducing a fictitious time t and unit velocity in the (x, y, a) space, we have $D_x G \cdot \dot{x} + D_y G \cdot \dot{y} + D_a G \cdot \dot{a} = 0$, $\dot{x}^2 + \dot{y}^2 + \dot{a}^2 = 1$. We obtain $D_{x,y}G$ and $D_a G$ from the recurrent formulas

$$D_{x,y}G = M_{n-1} \circ M_{n-2} \circ \cdots \circ M_0 - I$$

where

$$M_k = \begin{pmatrix} -2ax_k & 1 \\ b & 0 \end{pmatrix} \quad \text{if} \quad \begin{pmatrix} x_k \\ y_k \end{pmatrix} = T^k \begin{pmatrix} x \\ y \end{pmatrix}$$

and

$$D_a G = D_a T_a^n$$

$$D_a T_a^k = \begin{pmatrix} -x_{k-1}^2 \\ 0 \end{pmatrix} + \begin{pmatrix} -2ax_{k-1} & 1 \\ b & 0 \end{pmatrix} D_a T_a^{k-1}, \qquad k = 1 \text{ to } n$$

Certainly $|D_{x,y}G|$ can be zero (when one of the eigenvalues of T^n equals $+1$), but the quadratic behavior of the solutions with respect to a ensures that the rank of $D_{x,y,a}G$ equals 2 when $|D_{x,y}G| = 0$ if the point (x, y) does not have period $n/2$ for that value of a. Then there are no numerical difficulties in the continuation of the family of POs.

Unfortunately, when (x, y) has period $n/2$ we have a cubic behavior and rank $D_{x,y,a}G = 1$. Numerical continuation can be done by symmetry around the critical point (x, y, a) or by an analysis of the second differential. Via a local diffeomorphism mapping the characteristic curve $x(a)$, $y(a)$ into the real line we can use the ideas of Guckenheimer.[6]

Table III gives some periodic points that we can add to those of Table II. In Fig. 4 we plot some evolutions $x(a)$, $y(a)$ for different periodic points.

An n-periodic orbit is attracting if both eigenvalues have modulus less than one. As $|\lambda_1| \cdot |\lambda_2| = |(-b)^n| < 1$, stability is initiated when $\lambda_1 = 1$ and ends when $\lambda_2 = -1$. When $\lambda_1 = 1$ we have a bifurcation. An attracting and an unstable PO are created simultaneously. The value $\lambda_2 = -1$ means that

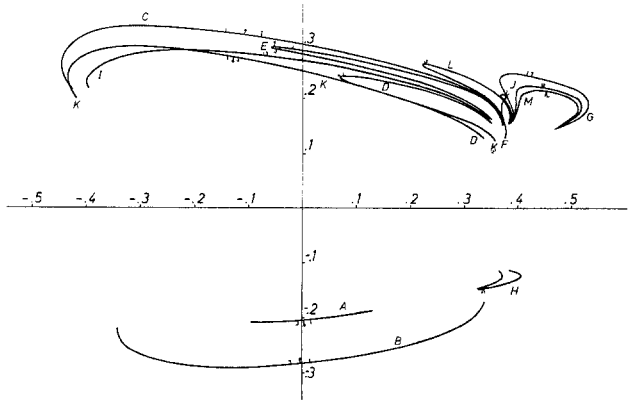

Fig. 4. Some periodic points as a function of a for $a \leqslant 2.8$. |: points with $\lambda_1 = 1$; ⌉: points with $\lambda_2 = -1$; ⁞: points with $|\lambda_1| = |\lambda_2|$. Associated values of a_k (see Table IV): 2.6575, 1.5239, 1.0624, 1.4492, 1.2266, 1.2991, 1.1218, 1.3233, 1.3866, 1.2940, 1.1001, 1.1768, 1.3904 for plots A–M, respectively.

Table III. Additional Periodic Points and One of the Associated Eigenvalues

a	Period	x	y	λ
1.07	4 (1 × 2²)	−0.00175651	0.25832047	−1.81586
1.07	6	0.34860969	0.18212252	−0.864962
1.07	6	0.29885794	0.19507916	2.75279
1.0720	12	0.12813633	0.23307435	0.390865
1.0731	12 (6 × 2)	0.36360154	0.17795670	−0.199089
1.0731	24 (12 × 2)	0.13183075	0.23222002	0.966407
1.143	20 (10 × 2)	0.42704961	0.24319591	0.388272
1.173	9	0.42751264	0.23934511	−1.55267
1.173	72 (9 × 2³)	0.42459872	0.23976637	−0.016858
1.177	20 (10 × 2)	0.22754463	0.26434875	−1.39128
1.23	7	0.42852339	0.38717441	0.119228
1.23	7	0.45152597	0.28621935	2.67339
1.25023	22 (11 × 2)	0.36360154	0.17795669	0.970098
1.26	14 (7 × 2)	0.41381333	0.20021787	−0.994825
1.2618	28 (7 × 2²)	0.40848823	0.20209616	−1.55846
1.262	14 (7 × 2)	0.41177966	0.20057558	−1.6879
1.300434	7	0.37589127	0.20728574	−0.014789
1.300434	7	0.37747700	0.20517803	1.95097
1.354	13	0.15110367	0.24001993	−0.756565
1.4	27	0.27154379	0.20553789	−14928.2
1.422	15	0.16835872	0.23607548	−0.943756
1.6	6	0.20274833	0.22184159	33.2707
2.6577	3	0.01043545	−0.20394794	0.685677
2.6577	5	0.36770208	0.15755829	136.94

T^{2n} has an eigenvalue 1. Two stable $2n$-periodic points are created, both belonging to some $2n$-periodic orbit, and the initial n-periodic point loses its stability. Therefore the numerical difficulties mentioned above are not essential. We can recover the lost half of the characteristic curve through iteration of T to one-half of the period.

As noted in Section 2.3, it seems that for $a = 1.4$ all the periods are present with the exception of $n = 3, 5$. Feit has made a search for 3-periodic orbits, because of the importance of period three (see Li and Yorke[10]). Points 3-periodic start at the exact value $a = 2.6575$ and are attracting until 2.664446.... The associated attractors can be seen in Ref. 5.

In the range $a \in [1.4269..., 2.6575]$ there can be found many attracting POs. For instance, at $a \simeq 1.4492292801$ there begins a 6-PO which remains attractive until $a \simeq 1.4508126$, when a 12-PO appears.

Another very interesting case is the 5-PO, which appears at $a \simeq 1.52394843$ and loses its attracting character at $a \simeq 1.527538$.

Once a PO is created for a given value of $a = a_0$ it remains for all other values $a > a_0$ (at least this has been observed in our experience; see Section 5.3). If the λ of maximum modulus is -1, that eigenvalue decreases monotonically. If it is 1, there is a transition to -1 in a certain interval $[a_0, a_0']$ (see Section 4.2). When we reach $\lambda = -1$, that eigenvalue again decreases monotonically.

3.3. Lyapunov Numbers and the Evolution of Attractors

In our case (R^2) we consider the limit $l = \lim_{n\to\infty}(1/n) \ln|\text{Spec } DT^n(x)|$ if it exists. Here Spec means the spectrum. As $|DT^n| = (-b)^n$, the two values taken by the lim exist simultaneously and are related by $l_1 + l_2 = \ln b$. They are called Lyapunov numbers or characteristic exponents associated with T. As the dimension is two, we shall call them maximal, l_1, and minimal, l_2, Lyapunov numbers. We refer to Pesin[14] for a general theorey of the Lyapunov numbers.

The meaning of the maximal Lyapunov number is the log of the maximum averaged rate of growth of the length of a vector under iterates of DT, starting at the point x, i.e., the velocity of separation of an orbit that begins at a point very close to x. If x belongs to a closed k-periodic orbit, then $l = (1/k) \ln|\text{Spec } DT^k(x)|$. The same is true if the PO attracts x. In this case $|\text{Spec } DT^k(y)| < 1$ ($y \in \text{PO}$) and $l < 0$.

The minimum value of l_1 is $\frac{1}{2} \ln b = -0.6019864$. Bifurcations are produced when $l_1 = 0$. Positive values of l_1 are associated with strange attractors.

We remark that different initial points may be attracted by different attractors. Then their ultimate behavior and, correspondingly, their characteristic exponents depend on the basin of attraction to which it belongs. For a

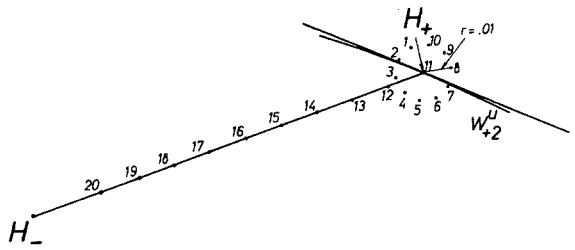

Fig. 5. Starting points for the evaluation of the Lyapunov numbers (for every value of a). Point 1 in the symmetric of the tangent to W^u_+ with respect to the line $x = y$. Add small displacements $\Delta x = \Delta y = 10^{-16}$.

fixed value of a many different attractors can exist and the associated Lyapunov numbers can be different (see Section 5.2). For points in the same basin the Lyapunov numbers are the same. Such basins are determined using stable manifolds of POs.

We restrict ourselves to points in the stable region R. For points outside this region $(1/n)\ln|\text{Spec } DT^n|$ has a diverging exponential behavior.

The effective computation of l_1 was done for every value of a, starting from 20 different points (Fig. 5). Ten of them were chosen equally spaced on a circumference of radius 0.01 around H_+. The others were along the line joining H_+ to H_-. Small perturbations $O(10^{-16})$ were added to these points. Then we computed T^n, DT^n up to $n = 15{,}000$. We supposed that for this value we were already near the attractor and obtained T^n, DT^n for $n = 15{,}001$–$30{,}000$. The adopted value of l_1 is the mean value for the last 15,000 iterations: $(1/15{,}000)\ln \max|\text{Spec } DT^{15{,}000}(T^{15{,}000}(x))|$. The 20 values obtained can differ for two reasons: the initial points tended to different attractors or the transient regime was not yet finished. When the last circumstance was suspected we increased the number of iterations up to a maximum of 450,000.

For most of the values of a, if $l_1 < 0$ for several starting points, the values of l_1 obtained (for the same attractor) agree to four decimal places. If $l_1 > 0$ there are minor errors $[O(10^{-3})]$ and the given values are averages. When an attracting k-PO is established, l_1 decreases (for increasing a) from zero at $a = a_k^i$ to $0.5 \ln 0.3$, then increases to zero at $a = a^i_{2\cdot k}$, and again we have a decrease corresponding to bifurcation. This pattern is repeated an infinity of times with decreasing widths in the a intervals (see Section 4.2). The values of a when $l_1 = 0$ (bifurcations) will be called a^i_k, $a^i_{2\cdot k}$, $a^i_{2^2\cdot k}$,..., $a^i_{2^n\cdot k}$,.... They accumulate at some value $a^i_{2^\infty\cdot k}$. The superscript i means that different attracting k-POs with the same basic k period can occur for different values of a.

Figure 6 gives a plot of the values of l_1 obtained for $a \in [1, 1.426]$. Several values of l_1 are associated with certain a values and the results are not com-

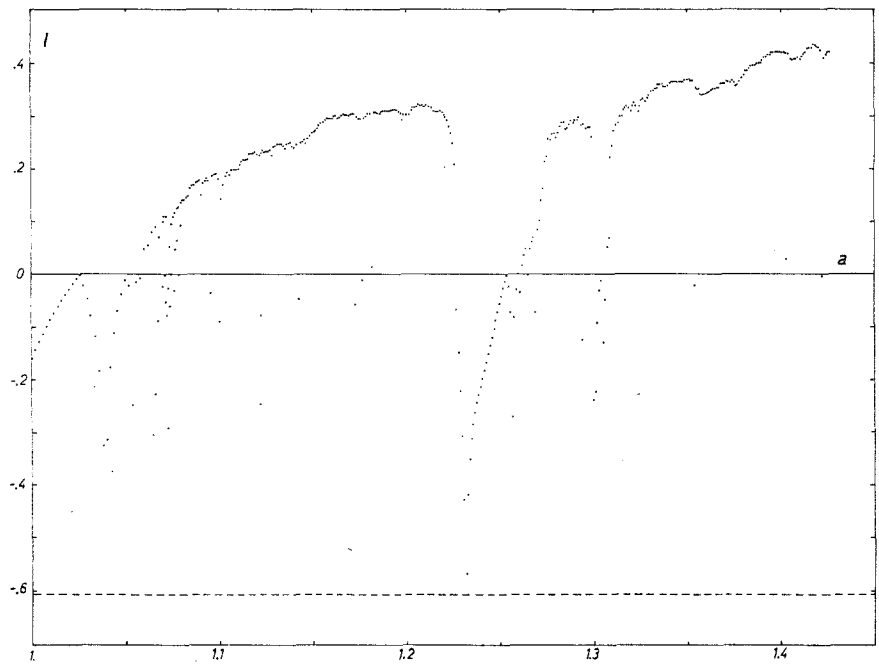

Fig. 6. Lyapunov numbers found starting at the points of Fig. 5.

plete. Other values can be obtained starting from other points. For instance, at $a = 1.0720$ we detected one SA with $l_1 = 0.109$ which attracts the points labeled 1, 3, 4, 7, 8, 9, 10, 11, 12, 15, 16, 18, 20; a 12-PO with $l_1 = -0.0521$, attracting the points 5, 6, 14, 17, 19; and another 12-PO with $l_1 = -0.0783$ attracting the points 2, 13. The SA has four pieces and is destroyed at $a \simeq 1.0723$. The previous history of that attractor is described in Section 3.1. The first 12-PO is obtained by bifurcation of an attracting 6-PO (whose birth is at $a \simeq 1.062371846$) at $a \simeq 1.071065$ and loses its attracting character at $a \simeq 1.07501$, where it bifurcates to 24-PO, then to 48-PO, etc. Accumulation of bifurcations takes place at 1.0763... and then it seems that a strange attractor with six pieces is born (see Section 4.5). The points attracted by such POs change to numbers 6, 14, 17, 19 at $a = 1.0732$, to 6, 11, 14, 17, 19 at $a = 1.0753$, and to 2, 6, 11, 14, 17, 19 at $a = 1.0763$. When the SA is born it attracts the same points.

On the other hand, the other 12-PO is born at $a \simeq 1.071902$ (not by bifurcation of a 6-PO; see Section 3.2) and for $a = 1.0720$ it attracts points 2, 13. Using the methods of Section 3.2, we can follow such a PO, but we lose it if we only consider Lyapunov numbers. Studying the Lyapunov numbers, we recover it at $a = 1.0724$. Then it produces the destruction of the four-

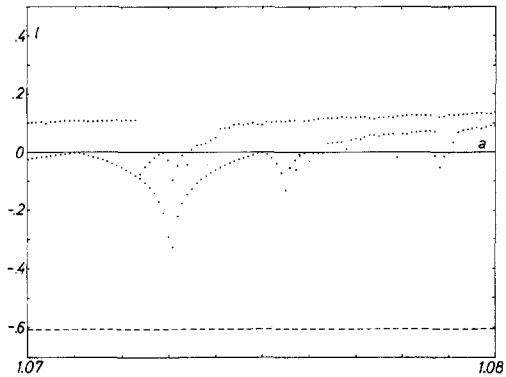

Fig. 7. Enlargement of Fig. 6 in the interval [1.07, 1.08].

piece SA and all the points (except numbers 5, 6, 14, 17, 19) are attracted by such a PO. A bifurcation to 24-PO occurs for $a \simeq 1.0729$, and successive bifurcations accumulate near $a = 1.0735$. After that value a SA is born. For $a = 1.0752$, for instance, we have one SA of four pieces (with $l_1 = 0.102$) and a 24-PO with $l_1 = -0.0208$ and we agree with Ref. 5. See Fig. 7 for $a \in$ [1.07, 1.08].

From $a = 1.0764$ on, two strange attractors are present with six pieces (attracting points 2, 6, 11, 14, 17, 19) and four pieces (attracting the remaining 14 points). Doing the computations with a step in a of 10^{-4} we found that the strange character of the two types of attractors can change in small intervals. The four-piece attractor is changed to a PO at $a = 1.0758$, 1.0787. The six-piece one is changed to an attracting PO at $a = 1.07674$, $a = 1.0779$, $a =$ 1.0788 to 1.0790 and disappears for $a \simeq 1.0806$. When one such SA is changed to a PO the attracted points are roughly the same. Those points change slowly with a. Partial results in [1.07, 1.08] are given by Curry.[3]

After the value $a = 1.081$ only the four-piece SA persists and changes to a two-piece SA as stated in Section 3.1 (roughly at $a = 1.084$). It is fully destroyed by PO at $a = 1.096$, $a = 1.101$, and $a = 1.143$. It exists but some of the points are attracted by a PO for $a = 1.122$ (points 2, 3, 18) and $a =$ 1.123(points 2, 3, 9, 18).

The two pieces of SA become only one piece for $a = a_{c1} \simeq 1.1535702$. Then the genuine Hénon–Pomeau attractor begins. Of course every attracting PO calls for a complete sequence of bifurcations and many POs have not been detected in that search.

After a_{c1} the SA is destroyed at $a = 1.173$, 1.177, 1.1770103, 1.177041, 1.1770595, 1.18199, among others, by different families of POs. At specific values of a many computations are done with rather small steps. The information is not described here but will be used in Section 4. In such regions we

increase the number of iterations in order to get a reliable value of l_1. The main difficulties in obtaining agreement between the l_1 values coming from different starting points are produced just in the regions of great change in l_1, especially after an accumulation of bifurcations is produced. Tentative reasons are given in Section 4.5.

At $a \simeq 1.2266173785$ there begins an attracting 7-PO which attracts all the points in R. The bifurcation at $a \simeq 1.24519$ gives rise to 14-PO, that at 1.260... to 28-PO, etc. After that we see a seven-piece SA destroyed at 1.265, 1.269 by POs, that is, changed again to the Hénon–Pomeau attractor for $a \simeq 1.273$. We have again destruction by 9-PO at 1.29395482337 and by 7-PO and bifurcations from $a = 1.2991160531$ to 1.306.... For a small range of values of a there is a seven-piece SA and at $a = 1.309$ the one-piece Hénon–Pomeau strange attractor reappears. This attractor exists until $a = a_{c2} = 1.4269212...$ (see Section 4.1), which is destroyed for very thin intervals of a near 1.354, 1.4028, 1.4219, among others. For $a = 1.4221$ we get a 15-piece SA. The value of l_1 is 0.011. Every one of the pieces is rather small and the global behavior is like that of an attracting PO which has just lost the attracting character. This explains the small value of l_1 because at the accumulation of bifurcations $a_{2^\infty \cdot 15}$ we get $l_1 = 0$.

4. EXPLAINING THE RESULTS

The information we have obtained through the previous computations gives us a rough idea of the complexity of the studied map. This calls for mechanisms to explain the observed phenomena, and this is the object of this section.

4.1. Unstable Invariant Manifolds As Strange Attractors

From Section 2 it seems that the closure of W_+^u is the SA. However, if W_+^u has to be an attractor, we must have the feedback property, i.e., we must have homoclinic points (similar ideas are found already in Newhouse[13]). The appearance of homoclinic points can be easily determined using the local expressions for $W_+^{u,s}$ and the continuation of W_+^u (we can restrict ourselves to a small piece of W_+^s near H_+). We have found the value $a = a_{c1} = 1.1535702...$ as the first critical value of a associated with the Hénon–Pomeau strange attractor.

In Fig. 8 we plot $W^{u,s}$ for $a = 1.1$, 1.2, 1.4, and 1.5.

We have already mentioned the (possible) existence of outer heteroclinic points: $W_+^u \cap W_-^s \neq \varnothing$. When transverse outer heteroclinic points exist there are pieces of W_+^u outside R. Points that initially become attracted by W_+^u are scattered along a thin neighborhood of such a manifold until they

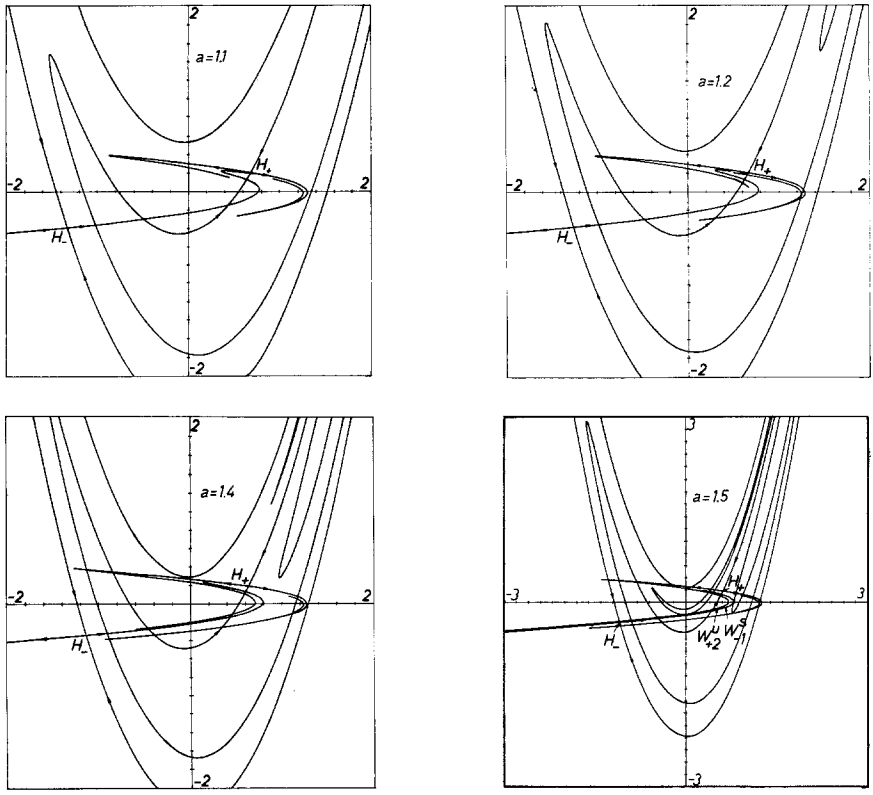

Fig. 8. Quantitative plots of $W^{u,s}_{\pm}$ for $a = 1.1$, 1.2, 1.4, 1.5. Here $W^{u}_{+} \cap W^{s}_{+} = \varnothing$ only for $a = 1.1$, and $W^{u}_{+} \cap W^{s}_{-} \neq \varnothing$ only for $a = 1.5$.

reach an outer region between two heteroclinic points (see Fig. 9). Then they become unstable. In our case the first appearance of an outer heteroclinic point is at $a = a_{c2} = 1.4269212...$, when the Hénon–Pomeau attractor disappears.

We can suggest that in general if an unstable invariant manifold has homoclinic points and no heteroclinic points and is bounded, then its closure is a strange attractor.

The same mechanisms explain the existence (or not) of strange attractors as the closure of invariant unstable manifolds of POs. For instance, when the 4-POs have associated homoclinic points, there is the possibility of $W^{u}_{4\text{-PO}}$ being the four pieces of a SA. However, when $W^{u}_{4\text{-PO}}$ cuts $W^{s}_{2\text{-PO}}$ the points obtained play the role of outer heteroclinic points and $W^{u}_{4\text{-PO}}$ loses its attracting character. Just at the same value the homoclinic points of $W^{u}_{2\text{-PO}}$ begin. Then the four-piece SA is converted to a two-piece SA (see Section 4.4).

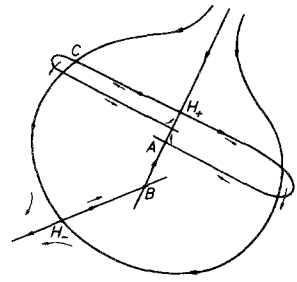

Fig. 9. Mechanism producing the escape for the points in the basin of W^u_+ when an outer heteroclinic point is present. Points: A, homoclinic; B, inner heteroclinic; C, outer heteroclinic.

4.2. The Evolution of POs

At some definite value a_k a k-PO begins. Let λ_1, λ_2 be the associated eigenvalues. We have $\lambda_1\lambda_2 = (-0.3)^k$. Suppose $\lambda_1(a_k) = 1$. We must distinguish the cases k odd and k even.

If k is odd, $\lambda_2 < 0$. At some value $a_k^{\min}$ we have $\lambda_1 = -\lambda_2 = (0.3)^{k/2}$. In $(a_k, a_k^{\min})$, l_1 is monotonically decreasing. From $a_k^{\min}$ on, $|\lambda_2| > |\lambda_1|$, l_1 increases again, and for $a = a_{2\cdot k}$ we get $\lambda_2 = -1$ and bifurcation appears.

If k is even, $\lambda_2(a_k) > 0$. In order to reach the value $\lambda_2(a_{2\cdot k}) = -1$ for the bifurcation we pass through complex values. From a_k to $a_k^{\min 1}$, $\lambda_1 \downarrow$, $\lambda_2 \uparrow$. At $a_k^{\min 1}$ we have $\lambda_1 = \lambda_2$ and a narrow band begins with $|\lambda_1| = |\lambda_2|$, both complex, which ends with $\lambda_1 = \lambda_2 < 0$ at $a = a_k^{\min 2}$. Then again $|\lambda_1| \downarrow$, $|\lambda_2| \uparrow$ up to $a = a_{2\cdot k}$. In $[a_k^{\min 1}, a_k^{\min 2}]$ the Lyapunov number equals the

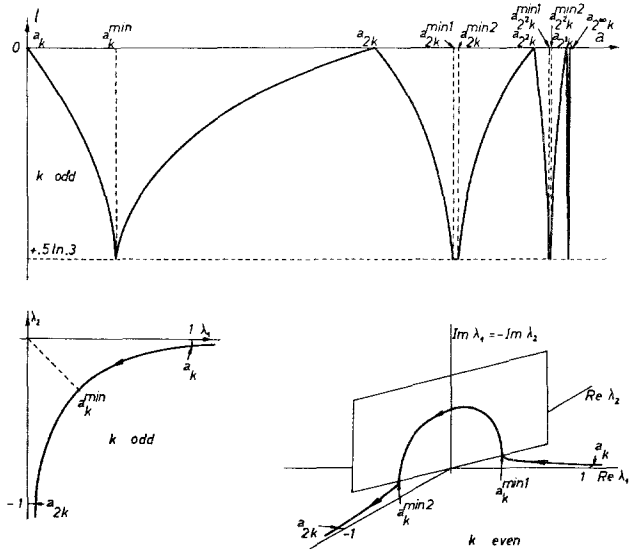

Fig. 10. Evolution of the Lyapunov number for the successive bifurcations of periodic orbits and of the eigenvalues between two consecutive bifurcations.

Table IV. Characteristics of Some Families of Periodic Orbits

k	j	$a_{k\cdot 2^j}$ ($\lambda_1 = 1$)	$a^{\min}_{k\cdot 2^j}$ ($\lvert\lambda\rvert$ = min) or $a^{\min 1}_{k\cdot 2^j} - a^{\min 2}_{k\cdot 2^j}$	$a_{k\cdot 2^{j+1}}$ ($\lambda_2 = -1$)
1	2	0.9125	0.960–0.979	1.025856
1	3	1.025856	1.039_{-}–1.039_{+}	1.051125
3	0	2.6575	2.659275	2.664446
5	0	1.52394843	1.524849	1.527537
6	0	1.062371846	1.0647_{-}–1.0647_{+}	1.071070
6	1	1.071070	1.0728_{-}–1.0728_{+}	1.07501
6	0	1.4492292801	1.449589–1.449661	1.4508126
7	0	1.2266173785	1.231845	1.25418337
7	1	1.25418337	1.257067–1.257070	1.260017
7	0	1.2991160531	1.300434	1.3038219
8	0	1.1218357533	1.122053–1.122065	1.1227199
8	0	1.32330679028	1.3233600–1.3233633	1.3235260
8	0	1.38661224376	1.38662488–1.38662570	1.3866643
9	0	1.172389	1.1725	1.172761
9	3	1.172994844	1.1729999_{-}–1.1729999_{+}	1.1730048
9	0	1.29395482337	1.29398045	1.29405702
10	0	1.10012012667	1.1003024–1.1003055	1.1008496
10	1	1.14298441	1.14301_{-}–1.14301_{+}	1.43035514
10	0	1.17676498357	1.1768016–1.1768023	1.1769123
10	1	1.1769123	1.1769492465–1.1769492469	1.1769856
10	0	1.39044286145	1.390443588–1.390443600	1.390445794
11	0	1.25018859547	1.25019876	1.2502293
12	0	1.07190193	1.07216_{-}–1.07216_{+}	1.0728902
12	1	1.0728902	1.07312_{-}–1.07312_{+}	1.07335
13	0	1.353917	1.353949	1.354055
13	0	1.39270600339	1.3927060175	1.39270605985
13	0	1.39944961920	1.39945236	1.39946057
15	0	1.368201373	1.368201406	1.368201496
15	0	1.38303779472	1.38303787896	1.38303813176
15	0	1.421812	1.42186	1.422008
19	0	1.39311487446	1.39311487505	1.39311487684
19	0	1.39614754924	1.39614754960	1.39614755068
21	0	1.39870159504	1.39870159508	1.39870159519
23	0	1.396095714617	1.396095714624	1.396095714643

minimum value. The pattern described for k even is the same as the one we have for the successive families of POs that bifurcate at $a_{2\cdot k}$, $a_{2^2\cdot k}$,.... Using the ideas similar to those of May and Oster,[12] we obtain that $(a_k^{\min} - a_k)/(a_{2\cdot k} - a_k^{\min})$ [or $(a_k^{\min 1} - a_k)/(a_{2\cdot k} - a_k^{\min 2})$ if k is even] is roughly equal to 3 (especially if k is high). Moreover, for the successive bifurcations $a_{2^j\cdot k}^{\min 2} - a_{2^j\cdot k} \simeq a_{2^{j+1}\cdot k} - a_{2^j\cdot k}^{\min 2}$, which again agrees with Ref. 12. The relative width $(a_q^{\min 2} - q_q^{\min 1})/(a_{2\cdot q} - a_q)$ seems of the type $\alpha \exp(\beta q)$ with α, β ad hoc constants, whether q equals some k even or $q = 2^j \cdot k$.

Finally, the widths of the attracting regions have a geometrically decreasing character: $(a_{2^{j+2}\cdot k} - a_{2^{j+1}\cdot k})/(a_{2^{j+1}\cdot k} - a_{2^j\cdot k})$ tends toward 1/6. (With quadratic behavior we get 0.457, 0.191, 0.170 for $j = 1, 2, 3$, respectively).

Figure 10 shows some of the stated properties. Table IV gives numerical results for a variety of POs.

4.3. Creation of Attracting Regions for POs

When an attracting k-PO is created an unstable one appears. Let A and B be points in such orbits, respectively. One of the branches $W_{B,1}^{\mathrm{u}}$ of the unstable manifold of B is attracted by A. The stable manifold W_B^{s} encloses a region which tends toward $W_{B,1}^{\mathrm{u}}$ and subsequently to A.

If W_B^{s} cuts the current strange attractor S, whatever it is (some W_+^{u} or $W_{n\text{-OP}}^{\mathrm{u}}$), the intersecting points play the role of outer heteroclinic points and destroy the SA. However, we do not lose stability; we merely transfer to the PO of A the attracting character of S. Figure 11 clarifies this. Figure 12 is a plot of the real behavior for $a = 1.300434$ (the reason for choosing such a value is that it is near an $a_7^{\min}$ and then has a great attracting force). The same idea can explain why if two SAs are present, one of them can destroy the other if outer heteroclinic points appear. That is the case for $a = 1.0806$ when the four-piece SA destroys the six-piece SA.

For $a = 1.07$ we have the plots of $W_{4;6\text{-PO}}^{\mathrm{s,u}}$ in Fig. 13. We cannot separate the invariant manifolds $W_{4\text{-PO}}^{\mathrm{u}}$ and $W_{6\text{-PO}}^{\mathrm{u}}$. The folds are so flat that they seem like only a line; for that reason we merely state where the more distant points reached by the manifolds are. We see clearly the homoclinic point for 4-PO, and the nonexistence of outer heteroclinic points: $W_{6\text{-PO}}^{\mathrm{s}} \cap W_{4\text{-PO}}^{\mathrm{u}} = \varnothing$. The

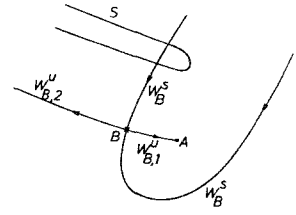

Fig. 11. Sketch of the destruction of a strange attractor by periodic orbits. S: previous SA; A: stable k-PO; B: unstable k-PO.

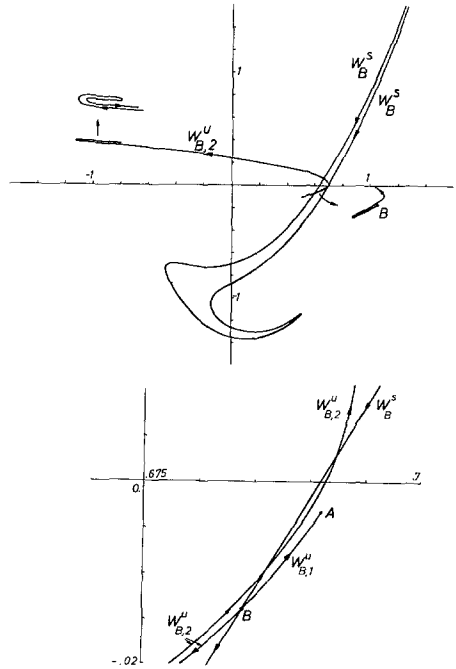

Fig. 12. Plot of an unstable 7-PO, B, for $a = 1.300434$, and the invariant manifolds. A is the attracting stable 7-PO with $|\lambda| \approx 0.3^{7/2}$.

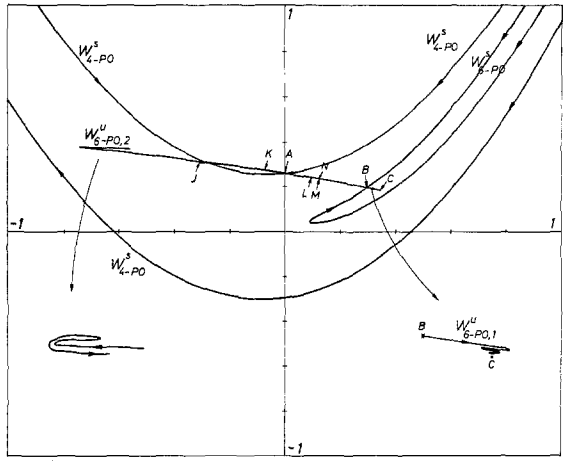

Fig. 13. Invariant manifolds for 4- and 6-POs. The value of a is 1.07. There is a four-piece strange attractor and an attracting 6-PO. Points: A, 4-periodic; B, unstable 6-periodic; C, stable 6-periodic; J, L, ends of the first two tongues of $W^u_{4\text{-PO},2}$; M, K, the same, for $W^u_{4\text{-PO},1}$; N, end of the second tongue of $W^u_{6\text{-PO},2}$. The strange attractor is roughly the arc JM.

attracting 6-PO enclosed between the two branches of $W^{s}_{6\text{-PO}}$ has some basin but does not destroy the four-piece SA. This explains the results in Section 3.1.

4.4. Fusion of Strange Attractors

We have seen that the genuine Hénon–Pomeau SA exists for $a \in (a_{c1}, a_{c2})$. However, for $1.058048 < a < a_{c1}$ there are periodic pieces of SAs. The value for which SAs initiate is a_{2^∞}. With a rough step in a (Section 3.1) eight-, four-, and two-piece SAs appear successively until $a = a_{c1}$. A finer search detects a 16-piece SA at $a = 1.059$, 32-piece SA at $a = 1.0582$, etc. (On the other hand, we get an attracting 16-PO at $a = 1.057$, 32-PO at $a = 1.0575$, 64-PO at $a = 1.0578$, 128-PO at $a = 1.058$, 256-PO at $a = 1.05804$, etc.)

In a similar way, after the successive bifurcations from the 7-PO which begins at $a = 1.2266173385$ we have a seven-piece SA at $a = 1.27$, but at $a = 1.262$ there is a 14-piece SA and we have detected a 28-piece SA at $a = 1.2619$, a 56-piece SA at $a = 1.26185$, and a 112-piece SA at $a = 1.2618$.

At some definite value of a the stable manifold of a $2^j \cdot k$-PO intersects for the first time both the unstable one and the unstable manifold of the $2^{j+1} \cdot k$-PO whose closure has been the SA up to this value. Then, as stated in 4.1, we lose the SA character of $W^{u}_{2^{j+1} \cdot k\text{-PO}}$, and $W^{u}_{2^j \cdot k\text{-PO}}$ gains it. We shall refer to this as the fusion of strange attractors.

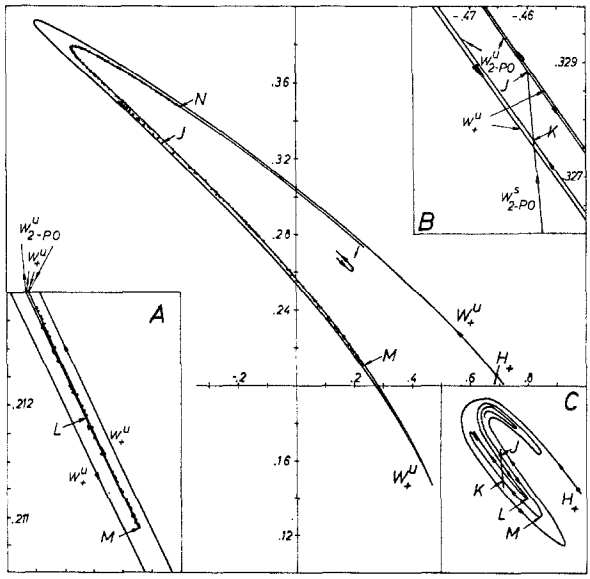

Fig. 14. Parameter $a = 1.1$. Strange attractor character for $W^{u}_{2\text{-PO}}$. Quantitative plot, two enlargements (A, B) and a qualitative picture (C). Points: J, 2-periodic; K, homoclinic for J; L, end of a tongue of W^{u}_{+}; M, N the same, for $W^{u}_{2\text{-PO}}$.

The existence of outer heteroclinic points leads to the fact that a $2k$-PO is a limit point of $W^{u}_{k\text{-PO}}$. If the k-PO has no homoclinic points but the $2k$-PO has, we have a $2k$-piece SA and not a k-piece SA. For the case $k = 1$, Fig. 14 shows some computations for $a = 1.1$. We show H_+, a 2-periodic point, and its unstable manifolds. In two enlargements we plot the behavior near the 2-PO point (including homoclinic and outer heteroclinic points) and a detail of one of the "extrema" of $W^{u}_{2\text{-PO}}$. The dots are iterates of an arbitrary initial point after the transient regime. This supports the evidence that $W^{u}_{2\text{-PO}}$ is the SA. A qualitative picture helps to understand the plots.

4.5. Accumulation of Bifurcations and Fusions

Two complementary phenomena have appeared: bifurcation of POs and fusion of SAs. The model that we propose unifies both facts.

When a given k-PO loses its stability through $\lambda_2 = -1$ a stable $2k$-PO appears, which, for increasing values of a, bifurcates again and again. The points of bifurcation accumulate at $a_{2^\infty \cdot k}$. Figure 15 shows the qualitative behavior (see also Ref. 10).

For a value of a slightly greater than $a_{2^\infty \cdot k}$ we have a k-piece SA (provided the conditions of Section 4.1 are satisfied). If we decrease a at some value $a^f_{2 \cdot k}$ every piece of the SA splits in two pieces of a $2k$-piece SA just as stated in Section 4.4. Successive decrements of a lead to new splittings at $a^f_{2^j \cdot k}$, $= 2, 3, \ldots$. We believe that the $a^f_{2^j \cdot k}$ accumulate at the same $a_{2^\infty \cdot k}$ as the bifurcations do. Figure 16 shows the evolution of attractors when a increases and crosses the critical value $a_{2^\infty \cdot k}$.

This model is also supported by the fact that just after $a_{2^\infty \cdot k}$, very small (positive) values of l_1 are obtained. They are associated with a SA with a large number of pieces.

Then a cascade of bifurcations of POs starting at a k-PO ends with the beginning of SAs that after some fusions develop a k-piece SA. The common

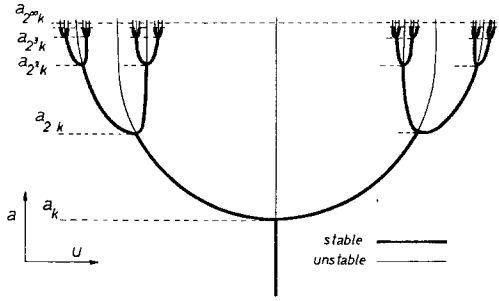

Fig. 15. Cascade of bifurcations of periodic points. The variable u is x, y, or some other variable used for the projection of the characteristic curve $x(a)$, $y(a)$.

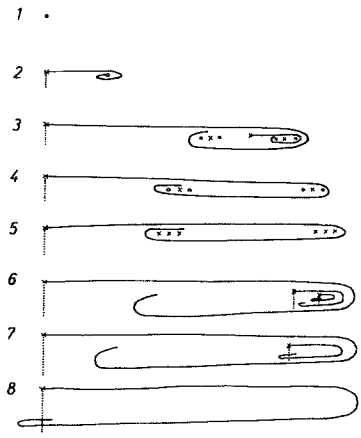

Fig. 16. Evolution of the attractor when a changes. (×) unstable point; (○) stable point; (——) part of unstable manifold; (· · ·) part of stable manifold. (1) Stable k-periodic point; (2) first bifurcation and unstable manifold; (3) third bifurcation; (4) high-order bifurcation; (5) critical value $a_{2^\infty k}$. All the bifurcates are unstable; (6) $W^{u}_{2^r k}$ is a strange attractor; (7) fusion of strange attractors. $W^{u}_{2^{r-1}k}$ becomes a SA; (8) after last fusion there is a k-piece SA.

feeling that the cascades of bifurcations or generalized catastrophes on the one hand and the strange attractors on the other have some relation with turbulence is supported by our numerical results: Both facts are the same!

We can say even more. We know[6,17] that for families of continuous maps of one interval into itself there is a definite order in the appearance of periodic points. It seems that this is true for the Hénon–Pomeau maps if the interval is replaced by some narrow band around W^{u}_{+}.

We must remark that the complicated fine structure is difficult to detect numerically. In fact, the origin of the difficulty is physical or geometrical. We can ask about the importance of the fine structure (see Ref. 1, p. 385). If we plot the attracting long periodic orbits and the many-piece SAs and do not enlarge the scale many times, what we see is almost a very small fuzzy set around periodic points of not very high order.

As noted in Section 4.2, asymptotic methods for high values of $2^j \cdot k$ can predict with great accuracy the values of a at the bifurcations and fusions of the $2^r \cdot k$-POs and $2^r \cdot k$-piece SAs ($r > j$) in terms of the greatest of the eigenvalues of the $2^j \cdot k$-PO.

5. ADDITIONAL REMARKS

We present here some remarks that complement the foregoing work.

5.1. Independent Computation of Lyapunov Numbers

The main part of the computations was the determination of Lyapunov numbers (in fact most of the remaining computations were done with a TI59 programmable pocket calculator). When there exists an attracting k-PO we have $l_1 = (1/k) \ln \max|\text{Spec } DT^k(Q)|$ if Q belongs to the k-PO. This is easily calculated along the families of POs obtained and agrees with the direct

evaluation. For strange attractors we can compute l_1 using only information along the associated W^u. Let σ be the arc parameter on W^u measured from the fixed (or periodic) point. Then l_1 is given by

$$l_1 = \lim_{s\to\infty} \int_0^s \ln\| DT|_{W^u}(x)\| \rho(x)\, d\sigma \Big/ \int_0^s \rho(x)\, d\sigma$$

where x are the points on W^u, $DT|_{W^u}$ is the differential of the map restricted to W^u, and $\|\cdots\|$ is the induced Euclidean norm. The function $\rho(x)$ is the density of limit points on W^u at x. We hope that in some cases it can be determined using a Frobenius–Perron algorithm as in Ref. 9.

Numerical experiments for computing l_1 using the above formula need some value for $\rho(x)$. Preliminary values are obtained taking a very small segment $\overline{P, TP}$ pn W^u near the fixed point, with a uniforming spacing on it, and iterating the points many times. Then $\rho(x)$ is roughly the number of points per unit of length. The convergence is rather slow toward the true value of l_1. Suppose that $l_1 > 0$ ($a = 1.4$ for example). As T is not orientation-preserving, we compute effectively with DT^2. Near the end of the fine tongues of W^u_{+1} the value of $\ln\| DT^2|_{W^u_{+1}}\|$ decreases to -1.8. Many points in the initial segment accumulate in such regions. This is the main reason for the slow rate of convergence.

We must remark that l_1 on W^u can be computed even if W^u has lost the SA character. The same is true for the Hausdorff dimension. When the SA is destroyed due to the action of attracting POs or of other SAs, it retains a latent character as attractor.

5.2. Hysteresis

As was observed by Feit and Curry, for a given value of a different attractors can be present simultaneously. Examples are given in Section 3 for which two SAs and POs coexist. Such a phenomenon is called hysteresis. If the behavior for the Hénon–Pomeau map is similar to the behavior of the Poincaré map of the Lorenz problem and if the properties of the Lorenz problem have some relation with those of Bénard's problem, then, depending on the history and for a given value of the Reynolds number, we can reach different turbulent regimes or quasiperiodic solutions.

5.3. Other Examples

In Ref. 2, Chirikov and Izraelev study dissipative maps, among them

$$T\begin{pmatrix} x \\ y \end{pmatrix} = \begin{pmatrix} x' \\ y' \end{pmatrix} = \begin{pmatrix} x + 9.76(yy - y + 1/6) - 0.3(x - 0.5) \\ y + x' - 0.5 \end{pmatrix} \pmod 1$$

In the line $x = 0$ of the two-dimensional torus the map is discontinuous. A

fine foliation of the phase space like the structures mentioned in Section 2.1 was found by Chirikov and Izraelev.

We found four fixed points for such a map: $x' = 0.5, 9.76(y^2 - y + 1/6) = 0$ and 1. All four points are hyperbolic (two of them with reflection). From the numerical experiments it seems that the attractor of the dissipative map coincides with the union of the four unstable invariant manifolds of the fixed points (even if such manifolds are discontinuous at the preimages of $x = 0$ as in our case).

Another interesting case worthy of mention is the one studied by Curry and Yorke.[4] The planar map is given by $\psi_2 \circ \psi_1$, where $\psi_1(\rho, \theta) = (\epsilon \ln(1 + \rho), \theta + 2)$ and $\psi_2(x, y) = (x, y + x^2)$, with ϵ a parameter greater than 1. The Jacobian is $\epsilon^2 \ln(1 + \rho)/\rho(1 + \rho)$. Then the map is expanding inside a given disk of radius $\rho = \rho(\epsilon)$ and contracting outside. At $\epsilon = 1.27277...$ a pair of stable–unstable 3-POs begins. Such orbits never bifurcate to 6-POs, but at $a = 1.3953...$ both branches meet again and the 3-POs disappear. It seems that in the full range of existence of 3-POs the stable one is the unique attractor.

For $\epsilon = 1.63$ we get a four-piece SA formed by the unstable manifolds of 4-periodic points [like (1.605221758, 2.485830278), $\lambda = -1.727498$]. When ϵ increases ($\lambda = -3.2733$ if $\epsilon = 1.7$) the four pieces interlace in a complicated way, appearing as a folded curve. Properties like the ones described by Hénon and Pomeau[7] are found if we enlarge the plots.

Decreasing ϵ offers a familiar panorama: $\epsilon = 1.6$ produces an attracting 8-PO, $\epsilon = 1.58$ an attracting 4-PO, etc. Four-periodic orbits disappear at $\epsilon = 1.52463....$

When ϵ equals 1.52 we found 7-PO [coming from $(-0.5936748927, -1.049918978)$, $\lambda = -2.382228$, for instance]. The $W^{u}_{7\text{-PO}}$ becomes the associated SA. If $\epsilon = 1.50$ the 7-PO has an attracting character. At the value $\epsilon = 1.49443...$ a fusion of the unstable and stable branches of the 7-PO is observed.

Successive families of 10-PO, 13-PO, 35-PO, etc., are found at $\epsilon = 1.49, 1.46, 1.45(1/3 > 11/35 > 4/13 > 3/10 > 1/4)$.

As a conclusion we think that in every case the mechanisms described in Section 4 (and others that do not play any role in the Hénon–Pomeau case) may be useful for understanding the structure of attractors. In any event, the location of homoclinic and heteroclinic points seems to be a key point.

REFERENCES

1. *Transformations ponctuelles et leurs applications* (CNRS Colloque 229; Toulouse, Septembre 1973; Editions du CNRS, 1976).
2. B. V. Chirikov and F. M. Izraelev, Some numerical experiments with a nonlinear mapping: stochastic component, in Ref. 1, pp. 409–428.

3. J. H. Curry, On the Hénon Transformation, preprint (1978).
4. J. H. Curry and J. A. Yorke, in *Lecture Notes in Math.*, No. 668 (Springer, 1978), pp. 48–66.
5. S. D. Feit, *Commun. Math. Phys.* **61**:249 (1978).
6. J. Guckenheimer, *Inventiones Math.* **39**:165 (1977).
7. M. Hénon and Y. Pomeau, in *Lecture Notes in Math.*, No. 565 (Springer, 1976), pp. 29–68.
8. J. P. Kahane, in *Lecture Notes in Math.*, No. 565 (Springer, 1976), pp. 94–103.
9. A. Lasota and J. A. Yorke, *Trans. Am. Math. Soc.* **186**:481 (1973).
10. T. Y. Li and J. A. Yorke, in *Dynamical Systems*, L. Cesari *et al.*, eds. (Academic, 1976), Vol. II, pp. 203–206.
11. E. N. Lorenz, *J. Atmos. Sci.* **20**:130 (1963).
12. R. M. May and G. F. Oster, *Am. Naturalist* **110**:573 (1976).
13. S. E. Newhouse, *Topology* **12**:9 (1974).
14. Ya. B. Pesin, *Russian Math. Surveys* **32**:55 (1977).
15. C. Simó, Atractores extraños, variedades invariantes y dimensión Hausdorff, *Jornadas Matemáticas Luso-Espanholas, Aveiro (Portugal)* (March 1978), to appear.
16. S. Smale, *Bull. Am. Math. Soc.* **73**:747 (1967).
17. P. Štefan, *Commun. Math. Phys.* **54**:237 (1977).